

# Aspects of in vitro fatigue in human cortical bone: time and cycle dependent crack growth

R.K. Nalla<sup>a</sup>, J.J. Kruzic<sup>a</sup>, J.H. Kinney<sup>b</sup>, R.O. Ritchie<sup>a,\*</sup>

<sup>a</sup> *Materials Sciences Division, Lawrence Berkeley National Laboratory, and Department of Materials Science and Engineering, University of California, Berkeley, CA 94720, USA*

<sup>b</sup> *Lawrence Livermore National Laboratory, Livermore, CA 94550, USA*

Received 20 February 2004; accepted 12 May 2004

Available online 8 July 2004

## Abstract

Although fatigue damage in bone induced by cyclic loading has been recognized as a problem of clinical significance, few fracture mechanics based studies have investigated how incipient cracks grow by fatigue in this material. In the present study, in vitro cyclic fatigue experiments were performed in order to quantify fatigue-crack growth behavior in human cortical bone. Crack-growth rates spanning five orders of magnitude were obtained for the extension of macroscopic cracks in the proximal-distal direction; growth-rate data could be well characterized by the linear-elastic stress-intensity range, using a simple (Paris) power law with exponents ranging from 4.4 to 9.5. Mechanistically, to discern whether such behavior results from “true” cyclic fatigue damage or is simply associated with a succession of quasi-static fracture events, cyclic crack-growth rates were compared to those measured under sustained (non-cyclic) loading. Measured fatigue-crack growth rates were found to exceed those “predicted” from the sustained load data at low growth rates ( $\sim 3 \times 10^{-10}$  to  $5 \times 10^{-7}$  m/cycle), suggesting that a “true” cyclic fatigue mechanism, such as alternating blunting and re-sharpening of the crack tip, is active in bone. Conversely, at higher growth rates ( $\sim 5 \times 10^{-7}$  to  $3 \times 10^{-5}$  m/cycle), the crack-growth data under sustained loads integrated over the loading cycle reasonably predicts the cyclic fatigue data, indicating that quasi-static fracture mechanisms predominate. The results are discussed in light of the occurrence of fatigue-related stress fractures in cortical bone.

© 2004 Elsevier Ltd. All rights reserved.

*Keywords:* Cortical bone; Fatigue; Fracture; Life prediction

## 1. Introduction

“Stress” fractures of human cortical bone are a well recognized clinical problem with incidence rates of 1–4% often being reported [1,2]; even higher rates are cited for adolescent athletes and military recruits [2–4]. Such fractures are believed to result from continued repetitive (cyclic fatigue) loading, rather than a single traumatic loading event. Stress fractures are commonly seen within a few weeks of a sudden increase in the loading patterns experienced by the bone, when the time elapsed is

insufficient for an adaptational response to alleviate the deleterious effects of the increased stress levels [2].

The traditional approach to studying the cyclic fatigue of bone has involved the so-called “stress-life” ( $S/N$ ) approach, wherein (nominally flaw-free) specimens are cycled at various load/stress levels in order to determine the number of cycles to failure. Indeed, most studies on the fatigue of cortical bone have been restricted to this approach (e.g., [5–21]) and have sought to investigate a wide variety of issues, such as age [13], donor species [9], cyclic frequency [12,14], testing geometry [14,15], loading mode [16–18], fatigue-induced damage accumulation [9,13,18–20], and its role in inducing in vivo repair (remodeling) and adaptation [21]. A mechanistic understanding of the details of fatigue damage in bone is clearly desirable if one is to understand which aspects of bone quality must be

\*Corresponding author. Department of Materials Science and Engineering, 381 Hearst Mining Building, University of California, Berkeley, CA 94720-1760, USA. Tel.: +1-510-486-5798; fax: +1-510-486-4881.

E-mail address: [RORitchie@lbl.gov](mailto:RORitchie@lbl.gov) (R.O. Ritchie).

targeted to reduce the risk of stress and fragility fractures, or minimize the deleterious effects of disease. However, with the *S/N* approach, the measured fatigue lifetime represents the number of the cycles both to initiate and propagate a (dominant) crack to failure; as a result, *S/N* fatigue results are difficult to interpret in terms of the mechanisms responsible for fatigue failure, as the factors affecting crack initiation and subsequent crack growth cannot readily be differentiated.

In the present work, we adopt a fracture mechanics approach to specifically examine the *propagation* of cracks of macroscopic (i.e., millimeter) dimensions in human cortical bone. This is deemed to be the more important aspect of fatigue damage, as bone is known to possess *in vivo* an inherent population of microcracks, which may minimize the role of the crack initiation stage. The approach requires a knowledge of the crack-propagation behavior in terms of the crack velocity,  $da/dt$ , or crack-growth rate per loading cycle,  $da/dN$ , as a function of, respectively, the linear-elastic (mode I) stress intensity,  $K$ , or range of stress intensity,  $\Delta K$ , in fatigue.<sup>1</sup>

Somewhat surprisingly, there have only been two studies to date that have looked at large-crack fatigue damage in bone in this manner [23,24], i.e., pertaining to the propagation of macroscopic, through-thickness, cracks of dimensions larger than a few millimeters.<sup>2</sup> The first of these, by Wright and Hayes [23], used longitudinally-oriented specimens of bovine bone to measure crack-growth rates over a relatively narrow range ( $\sim 7 \times 10^{-7}$  to  $\sim 3 \times 10^{-4}$  m/cycle) for  $\Delta K$  levels between 2.7 to 8  $\text{MPa}\sqrt{\text{m}}$ . These data were fitted to a simple Paris power-law formulation [26]:

$$da/dN = C(\Delta K)^m, \quad (1)$$

where  $C$  and  $m$  (Paris exponent) are scaling constants, and gave values of  $m$  between 2.8 to 5.1. Although their data did suggest some effect of cyclic frequency on crack-growth rates, their results were not conclusive; furthermore, it has subsequently been suggested that the bovine bone they used is most likely primary plexiform bone [24], which is very different microstructurally from human osteonal bone. A second study, by Gibeling et al. [24], reported crack-growth rates between  $\sim 6 \times 10^{-10}$  to  $\sim 1 \times 10^{-5}$  m/cycle, with a Paris exponent of  $m \sim 10$ , for transverse fatigue-crack growth in osteonal equine bone.

<sup>1</sup>The stress-intensity factor,  $K$ , is a global parameter that fully characterizes the local stress and deformation fields in the immediate vicinity of a crack tip in a linear elastic solid, and thus can be used to correlate to the extent of crack advance. It is defined for a crack of length  $a$  as  $K = Q\sigma_{\text{app}}(\pi a)^{1/2}$ , where  $\sigma_{\text{app}}$  is the applied stress and  $Q$  is a geometry factor of order unity [22].

<sup>2</sup>*Large crack* strictly refers to a macroscopic crack which is large (in width and in length) compared to the scale of microstructure. For a discussion of the relative behavior of large vs. small cracks in fatigue, the reader is referred to Ref. [25].

However, to our knowledge, no large-crack growth rates have ever been measured for human bone. There has been one study [27] that focused on the growth of small surface cracks in human bone, where crack sizes were small compared to the microstructural features, although the mechanisms of such small crack growth were not considered in that work.

In addition to characterizing the fatigue behavior in bone, from a mechanistic viewpoint it is important to discern whether crack growth is a unique consequence of the repetitive cycling, or due to a succession of quasi-static fracture events driven by the maximum load, i.e., whether the damage is cycle- or time-dependent. Although the susceptibility of ductile materials to fatigue is well known, in many brittle materials there is no *true* effect of cyclic loading, and mechanisms of failure under static and cyclic loading are essentially the same; here, fatigue cycling can be equated to a series of continually interrupted static tests (e.g., [28]). Such subcritical crack growth (static fatigue) under a sustained (non-cyclic) load has been reported for human cortical bone, as shown in Fig. 1 [29], where cracks were observed to propagate at velocities of  $\sim 2 \times 10^{-9}$  m/s at stress intensities some 35% below the crack-initiation toughness, according to the power-law relation:

$$da/dt = AK^n, \quad (2)$$

where  $A$  and  $n$  ( $\sim 21$ – $31$ ) are scaling constants.

One approach to ascertain if fatigue damage in bone is time- or cycle-dependent is to examine the role of test

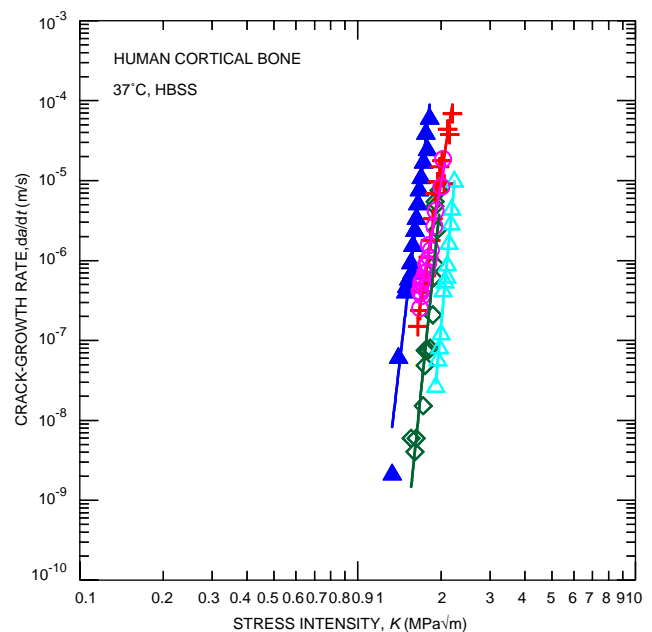


Fig. 1. Variation in subcritical crack-growth rates,  $da/dt$ , with the stress intensity  $K$ , for time-dependent *in vitro* cracking in the proximal-distal orientation in human cortical bone under sustained (non-cyclic) loads in 37°C HBSS (after Ref. [29]).

frequency on the stress-life behavior; a time-dependent mechanism is implied if the times-to-failure for different test frequencies are identical although the cycles-to-failure vary. Such an analysis of stress-life data from Caler and Carter [8], Lafferty and Raju [5], and Zioupos et al. [12] suggest that tensile fatigue in bone is actually time-dependent, since when plotted with respect to time, the effect of test frequency (0.002–2 Hz in [8], 30–125 Hz in [5], and 0.5–5 Hz in [12]) on the fatigue lifetimes is essentially eliminated. To explain these observations, Carter and Caler [7], and subsequently Taylor [2], have suggested that there is a transition in bone from a “creep”-dominated to a fatigue-dominated regime with decreasing stress levels. However, as failure times in fatigue-life experiments include both crack initiation and propagation stages, stress-life results are not easy to interpret. Furthermore, the crack growth approach allows for direct observation of the extension of cracks over a range of loading conditions, such that it can readily be ascertained whether there is any change in mechanism with loading. Consequently, in this work, we focus solely on crack growth in order to better differentiate between cyclic and static loading effects. Such an approach has been successfully used in brittle ceramics which may or may not be susceptible to true cyclic fatigue damage (e.g., [28, 30]).

Specifically, we characterize (for the first time) the *in vitro* fatigue-crack growth behavior of human cortical bone for the purpose of developing an understanding of the mechanism of fatigue, specifically in the proximal-distal direction, and seek to determine whether the fatigue damage is cycle- or time-dependent using three procedures: (i) by interrupting cyclic fatigue tests and holding at maximum load, (ii) by varying the frequency under constant cyclic loading conditions, and (iii) by comparing predictions based on sustained-load cracking data [29] (integrated over the fatigue loading cycle) with the measured cyclic fatigue-crack growth data. Results are used to interpret the susceptibility of human cortical bone to cyclic loading and to identify the salient damage mechanisms involved.

## 2. Materials and methods

### 2.1. Materials

Fresh frozen human cadaveric humeral cortical bone (donor age: 34–41 years, no known skeletal pathologies) was used in this study. Blocks of bone were obtained by carefully sectioning the mid-diaphyses of the left humeri taken from each of the four donors. Fourteen compact-tension, *C(T)*, specimens were machined from the humeri of four donors (Age(years)/sex: 34/female, 37/male, 37/male, 41/female);  $N = 1$  was from the 34-year old female,  $N = 11$  from the 37-year old males, and

$N = 2$  from the 41-year old female. Specimens were machined with a thickness,  $B \sim 2.2$ – $3.4$  mm, width,  $W \sim 13.6$ – $16.5$  mm and initial crack length,  $a \sim 2.5$ – $4.3$  mm, and were all orientated with the nominal crack-growth direction along the proximal-distal direction of the humerus, i.e., parallel to the long axis of the osteons (and hence, the humerus), as illustrated in Fig. 2a.

It should be noted that all specimen dimensions satisfied the ASTM Standard E647-00 for measurement of fatigue-crack growth rates [31]. There are no “plane strain vs. plane stress” requirements for the measurement of growth rates, and the standard recommends that specimens with  $W/20 \leq B \leq W/4$  be used, consistent with the current specimen dimensions. As these dimensions and crack sizes are all large compared to the scale of the microstructure, and there is no evidence of excessive “yielding”, we expect the results from these samples to be independent of specimen size. Furthermore, while it is recognized that based on expected physiological loading conditions, the transverse, and not longitudinal, cracking direction would seem to be the most relevant, cracks loaded so as to cause growth in the transverse direction *in vitro* have been found to deflect towards the longitudinal direction (e.g., [32]). Accordingly, in order to gain a mechanistic understanding of cortical bone fatigue, the longitudinal orientation would appear to be physiologically relevant. We have also used the longitudinal orientation to permit larger amounts of crack extension that would be possible in the transverse orientation.

The specimens were polished to a 1200 grit finish, followed by polishing steps using a 1  $\mu\text{m}$  alumina suspension and finally a 0.05  $\mu\text{m}$  alumina suspension. To facilitate crack initiation, the notch was first introduced with using a slow speed saw, and then was sharpened using a razor-micronotching technique. Specifically a micronotch, with root radius  $\sim 15 \mu\text{m}$ , was obtained by repeatedly sliding a razor blade over the saw-cut notch using a custom-made rig, while continually irrigating with a 1  $\mu\text{m}$  diamond slurry. The size and sharpness of the micronotch were subsequently verified using optical microscopy. Fatigue cracks were grown  $\sim 50 \mu\text{m}$  from the micronotch (i.e., a distance larger than at least two notch root radii) before data were collected in order to eliminate any effects of the notch field on subsequent growth rates.

### 2.2. Fatigue testing

Prior to testing, six of the *C(T)* specimens ( $N = 6$ ; mean age in years = 37.83 (S.D. = 2.71); see Table 1 for further details) were prepared by soaking in Hanks’ Balanced Salt Solution (HBSS) for at least 40 h at room temperature. All testing was conducted in HBSS (with gentamicin added to prevent specimen deterioration

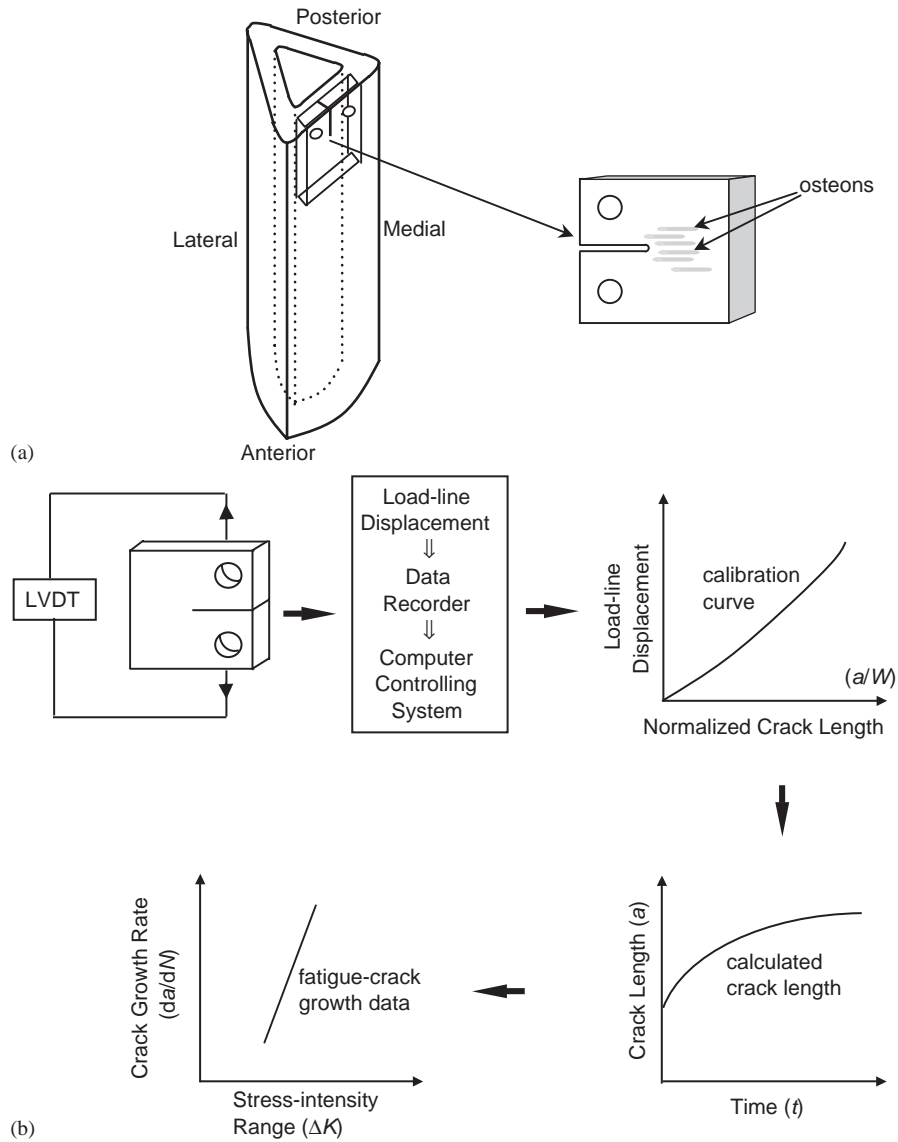


Fig. 2. Schematic illustrations of (a) the orientation of the compact-tension specimen taken from the human humeri to permit crack extension in the proximal-distal direction. (nominal orientation with respect to the osteons is also indicated), and (b) the experimental set-up used in this study to obtain the fatigue-crack growth data.

Table 1  
Paris Law Constants for Fatigue-Crack Growth in Human Cortical Bone

Donor Information <sup>a</sup>	Slope <sup>b</sup> <i>C</i>	Exponent <i>n</i>	Coefficient of determination ( <i>R</i> <sup>2</sup> )
34FL	$5.2 \times 10^{-8}$	7.8	0.96
37MLa#1	$4.1 \times 10^{-8}$	5.0	0.82
37MLa#2	$6.5 \times 10^{-8}$	6.0	0.95
37MLb#1	$3.7 \times 10^{-6}$	9.5	0.94
41FL	$2.65 \times 10^{-6}$	9.3	0.75
41FL	$2.3 \times 10^{-7}$	4.4	0.96
37MLa#3, #4, #5, #6 <sup>c</sup>			
37MLb#2, #3, #4, #5 <sup>c</sup>			

<sup>a</sup>The notation reads as follows: Age (years), Sex (M = Male, F = Female), Arm (L = Left, R = Right), with any subsequent letter being a unique identifier when more than one donor in an age group.

<sup>b</sup>units of (m/cycle) (MPam)<sup>-*n*</sup>.

<sup>c</sup>One specimen from each donor was used for each of the “fatigue/sustained load/ fatigue” and the “1 Hz fatigue/10 Hz fatigue/1 Hz fatigue” experiments.

from bacterial action) at  $37(\pm 0.5)^{\circ}\text{C}$ . Cyclic fatigue-crack growth testing was performed under load control using sinusoidal loading at 1 Hz frequency (unless otherwise stated) using a standard servo-hydraulic mechanical testing machine (MTS 810, MTS Systems Corporation, Eden Prairie, MN) in general accordance with ASTM Standard E-647 [31]; a constant load ratio of  $R = 0.1$  was maintained where  $R$  is the ratio of minimum to maximum load. Crack lengths,  $a$ , were monitored in situ using the elastic unloading compliance, i.e., the slope of the load-line displacement/load curve, with the load-line displacements measured using a linear variable-displacement transducer (LVDT) mounted in the load frame. Linear-elastic solutions for the relationship between compliance,  $C$ , and crack length,  $a$ , were taken from Ref. [33] and are given by

$$a/W = 1.0002 - 4.0632U + 11.242U^2 - 106.04U^3 + 464.33U^4 - 650.68U^5, \quad (3)$$

where  $U$  is a fitting function written as

$$U = \frac{1}{(FC)^{1/2} + 1}, \quad (4)$$

where  $C$  is the sample compliance and  $F$  is a calibration constant, taken to be that which gives the best agreement between the initial compliance and optically measured crack length at the beginning of the test. Fig. 2b illustrates schematically the set-up used for these tests. Because regions of intact material, termed crack bridges, are invariably left in the wake of the fatigue cracks, errors can be induced in the in situ crack-length measurements as these bridges clearly affect the sample compliance. Accordingly, periodic optical microscopy measurements were used to verify and correct the measured crack lengths by assuming that any such error accumulated linearly with crack extension. Further details on the use of compliance for crack-length monitoring are described in general in Ref. [31], and specifically for bone in Ref. [29].

In vitro fatigue-crack growth rates,  $da/dN$ , were characterized in terms of the stress-intensity range,  $\Delta K = K_{\max} - K_{\min}$ , where the maximum and minimum stress intensities,  $K_{\max}$  and  $K_{\min}$ , respectively, were computed from the maximum and minimum loads of the loading cycle using standard linear-elastic stress-intensity solutions [34]. In order to test over a range of  $\Delta K$ , the loads were continually adjusted such that  $\Delta K$  varied in a controlled manner, viz.:

$$\Delta K = \Delta K_{\text{initial}} \exp[C'(a - a_{\text{initial}})]. \quad (5)$$

The majority of the fatigue testing was performed under decreasing  $\Delta K$  conditions, with the  $K$ -gradient,  $C'$ , nominally set at  $-0.08 \text{ mm}^{-1}$ . However, at higher growth rates (roughly  $> 10^{-6} \text{ m/cycle}$ ), increasing  $\Delta K$  conditions, with  $C'$  nominally set at  $+0.08 \text{ mm}^{-1}$ , were

utilized.<sup>3</sup> Data for over five orders of magnitude of fatigue-crack growth rates ( $\sim 10^{-10}$  to  $\sim 10^{-5} \text{ m/cycle}$ ) were obtained. Fatigue thresholds,  $\Delta K_{\text{TH}}$ , below which cracking is presumed to be dormant, were operationally defined at growth rates of  $10^{-10} \text{ m/cycle}$ .

After fatigue testing, crack paths and fracture surfaces were examined using optical microscopy and scanning electron microscopy (SEM); SEM studies were performed in the secondary electron mode after coating the specimens with a gold-palladium alloy. Samples were kept hydrated until the coating process was performed.

### 2.3. Cyclic vs. static load and variable frequency tests

In order to ascertain the role of static versus cyclic fatigue mechanisms on subcritical crack growth in bone, three additional in vitro experiments were conducted on the remaining eight specimens. The first two experiments involved a three-step, “fatigue/sustained load/fatigue” regimen, with all three blocks performed at a fixed  $K_{\max}$  value:

- an initial block of cyclic fatigue loading at a constant  $\Delta K$  value ( $R = 0.1$ , 1 Hz)
- a second block of sustained loading at the maximum stress-intensity,  $K_{\max}$ , used in the previous fatigue loading block,
- a third block of cyclic loading identical to the first block.

Determining whether crack extension is motivated by the maximum or alternating loads (or both) can then be achieved by comparing the respective growth rates during static and cyclic loading at the same  $K_{\max}$ . Two  $\Delta K$  levels were used for the cyclic loading blocks; 1.5 and 0.9  $\text{MPa}\sqrt{\text{m}}$  (corresponding to a  $K_{\max}$  of 1.65 and 1  $\text{MPa}\sqrt{\text{m}}$ , respectively), with two specimens (donor age = 37 years) being tested under each condition. As with the fatigue testing, experiments were conducted in HBSS at  $37(\pm 0.5)^{\circ}\text{C}$ .

The final experiments involved changing the test frequency at a constant  $\Delta K$  level using a three-step, “1 Hz fatigue/10 Hz fatigue/1 Hz fatigue” regimen, akin to that described above with the middle block being of 10 Hz fatigue, instead of static loading. This experiment was also conducted at two  $\Delta K$  levels of 1.5 and 0.9  $\text{MPa}\sqrt{\text{m}}$ , ( $K_{\max} = 1.65$  and, 1  $\text{MPa}\sqrt{\text{m}}$ , respectively), on two specimens each to evaluate the effect of test frequency on growth-rate behavior from the perspective of improving mechanistic understanding. During these tests, crack extension was monitored using sample compliance as measured by the LVDT; as described above, corrections based on direct optical

<sup>3</sup>Such a  $K$ -gradient of  $\pm 0.08 \text{ mm}^{-1}$  is specified in ASTM Standard E647-00 [31] for the “Standard Test Method for Measurement of Fatigue Crack Growth Rates”.

measurements were made at the end of each loading block.

### 3. Results

#### 3.1. Fatigue-crack growth

The variation in fatigue-crack growth rates with stress-intensity range,  $\Delta K$ , based on results from the six  $C(T)$  specimens, is shown for human cortical bone in Fig. 3, with data spanning more than five orders of magnitude of growth rates from  $\sim 2 \times 10^{-10}$  to  $\sim 3 \times 10^{-5}$  m/cycle. Regression analysis of the data, to a Paris power-law formulation, was achieved using a least-squares power-law fit to Eq. (1); values of the scaling constants,  $C$  and  $m$ , for each individual specimen are listed in Table 1. The exponents,  $m \sim 4.4$ – $9.5$  obtained in this study, compare well to the range reported in previous work on bovine and equine bone [23, 24]. Fatigue thresholds,  $\Delta K_{TH}$ , were in the range 0.45 to 0.6  $\text{MPa}\sqrt{\text{m}}$ . Corresponding subcritical crack-velocity data for time-dependent cracking under sustained (non-cyclic) loads [29] is shown in Fig. 1.

#### 3.2. Fractographic observations

The fractography of fatigue-crack growth in human cortical bone is shown in Figs. 4 and 5. Fig. 4 shows

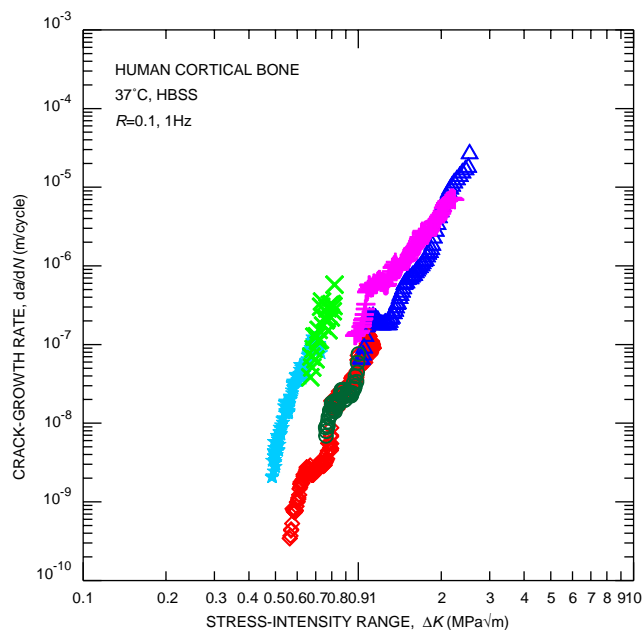


Fig. 3. Variation in in vitro fatigue-crack growth rates,  $da/dN$ , as a function of the stress-intensity range,  $\Delta K$ , for macroscopic cracking in the proximal-distal orientation in human cortical bone. All six data sets are included, each with a different symbol. All tests were performed at a load ratio of  $R = 0.1$  at 1 Hz frequency in 37°C HBSS.

optical micrographs of the trajectories of fatigue cracks emanating from notches at both low and high growth rates, i.e., at  $3 \times 10^{-10}$  and  $3 \times 10^{-7}$  m/cycle. The discontinuous nature of the crack path reveals the presence along the crack length of unbroken regions (termed “uncracked ligaments”), which act to bridge the crack, thereby increasing resistance to fracture by sustaining part of the applied load that would otherwise contribute to crack advance. These regions result from either non-uniform extension of the crack front, or where the main crack attempts to link-up with small cracks initiated ahead of the crack tip. On the sample surface, some of these “uncracked-ligament bridges” (indicated by white arrows) are as large as hundreds of micrometers in size. Also of note is the fact that the cracks do not appear to penetrate the bulk of the osteon at any stage; indeed, the path taken by the crack for this proximal-distal direction appears to be dictated by the cement line, i.e., the interface of the osteonal system with the surrounding matrix (see also Ref. [29]). The width of the crack, i.e., the crack-opening displacement, can also be seen to be substantially larger at the slower growth rates. This is consistent with previous observations that cracks in human cortical bone [29], as well as in dentin [35], experience a time-dependent crack-blunting phenomenon, as discussed below in Section 4. Such crack blunting was far less apparent at the higher crack-growth rates.

Corresponding scanning electron microscopy images of the fatigue fracture surfaces and final (overload) failure are shown in Fig. 5. Although the inherent complexity of the underlying microstructure can mask any distinction, at this magnification few differences appear to exist in the morphology of the fatigue (Fig. 5a) and overload (Fig. 5b) fractures, although macroscopically the overload fracture surfaces are somewhat rougher. Similar behavior has been reported for dentin [36,37].

#### 3.3. Cyclic vs. static load tests

To enhance mechanistic understanding, combined “fatigue/sustained load/fatigue” tests, as described in Section 2.3, were conducted at two specific (constant)  $K_{max}$  levels:

- $K_{max} = 1.65 \text{ MPa}\sqrt{\text{m}}$ , corresponding to a (higher) growth rate where limited crack blunting was seen (akin to top panel of Fig. 4), and
- $K_{max} = 1 \text{ MPa}\sqrt{\text{m}}$ , corresponding to a (lower) growth rate where appreciable crack blunting was apparent (akin to bottom panel of Fig. 4).

Representative crack extension ( $\Delta a$ ) vs. time ( $t$ ) data obtained for these two tests are shown in Figs. 6a and b. For a  $K_{max}$  of  $1.65 \text{ MPa}\sqrt{\text{m}}$ , crack growth was observed

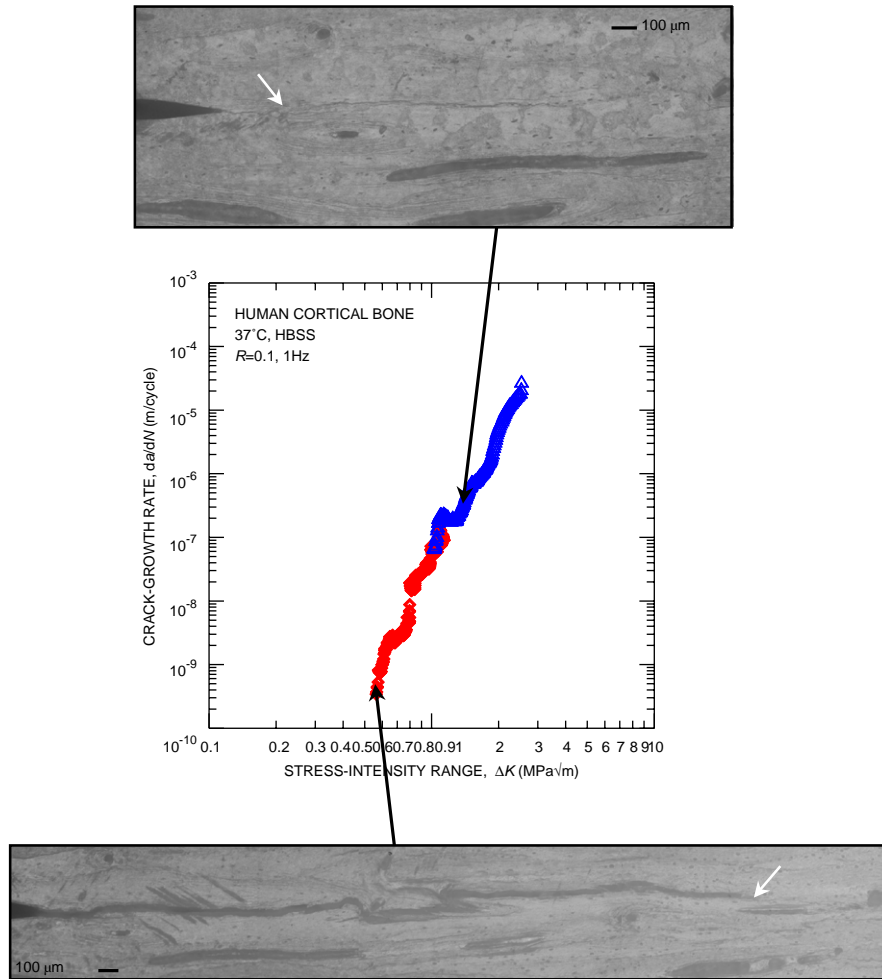


Fig. 4. Typical optical micrographs of the crack paths at fatigue-crack growth rates,  $da/dN$ , of  $3 \times 10^{-7}$  and  $3 \times 10^{-10}$  m/cycle. Nominal direction of crack growth is from left to right. The white arrows indicate uncracked ligaments in the crack wake. Note the much larger crack-opening displacements for the slower crack-growth rate.

during all three loading blocks, with crack velocities (with respect to time) being relatively similar whether or not the loading was sustained or cyclic (Fig. 6a). In contrast, at a  $K_{\max}$  of  $1 \text{ MPa}\sqrt{\text{m}}$ , subcritical crack growth was undetectable during the sustained-load portion, but restarted once the fatigue cycling was resumed (Fig. 6b). This strongly implies that at the lower growth rates (at a  $K_{\max}$  of  $1 \text{ MPa}\sqrt{\text{m}}$ ), it is not the maximum stress itself, but the process of fatigue cycling—repeated loading and unloading between the maximum and minimum stresses—that drives crack growth, i.e., subcritical cracking in bone in this low growth-rate regime is truly cycle-dependent. Conversely, at the higher growth rates, at a  $K_{\max}$  of  $1.65 \text{ MPa}\sqrt{\text{m}}$ , the magnitude of the maximum stress is high enough to drive crack growth in the absence of cycling, although cycling does seem to accelerate growth slightly as evidenced by a small increase in crack velocity upon the transition from loading block 2 (static) to loading block 3 (cyclic); this implies that subcritical cracking in

cortical bone in this higher growth-rate regime is both cycle- and time-dependent. Such results strongly support the notion of a “transition” in the salient mechanisms responsible for subcritical crack growth in bone, from static-load (or “creep”<sup>4</sup>) dominated to cyclic-load (fatigue) dominated mechanism(s), with decreasing growth rates and stress-intensity level.

### 3.4. Variable frequency tests

With respect to variations in cyclic frequency, Figs. 7a and b show representative crack extension ( $\Delta a$ ) vs. time ( $t$ ) data obtained for the constant- $\Delta K$  “1 Hz/10 Hz/1 Hz” tests, performed, respectively, at high ( $= 1.5 \text{ MPa}\sqrt{\text{m}}$ ), and low ( $= 0.9 \text{ MPa}\sqrt{\text{m}}$ )  $\Delta K$  levels, i.e., above and below the “transition” described above.

<sup>4</sup>While creep has been suggested as a possible static growth mechanism [2,7], the true mechanism for subcritical crack growth under sustained loads in bone is as yet unknown.

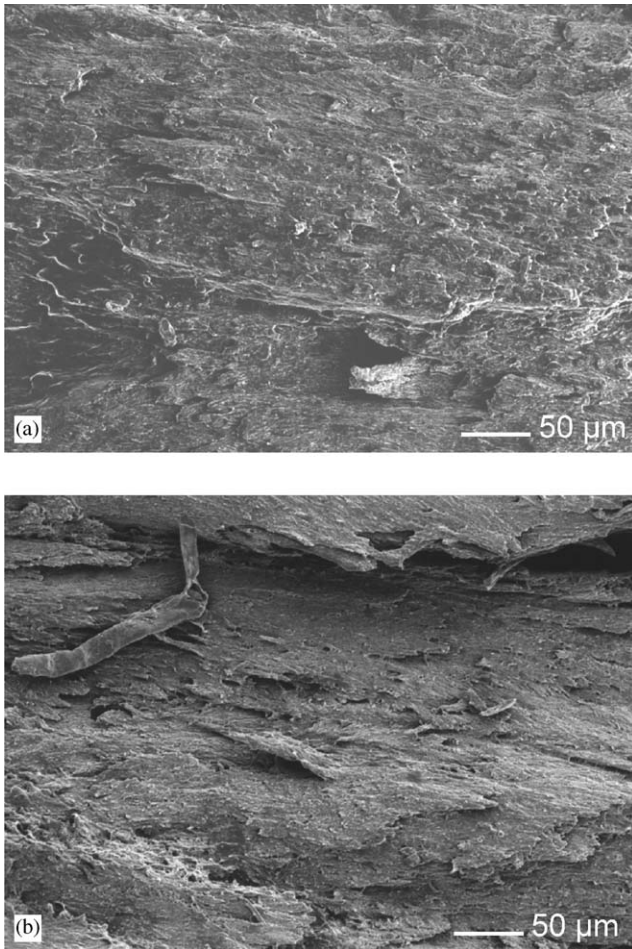


Fig. 5. Scanning electron micrographs of typical fracture surfaces associated with (a) cyclic fatigue ( $\Delta K = 0.95 \text{ MPa}\sqrt{\text{m}}$ ), and (b) overload fracture in human cortical bone tested in vitro. Note that the overload fracture surface appears macroscopically rougher.

From these experiments, it is clearly apparent that at the high  $\Delta K$  levels, growth rates, expressed in terms of  $da/dt$ , are comparable at both frequencies (Fig. 7a), consistent with a significant time-dependent contribution to crack growth. This is in contrast to the low  $\Delta K$  behavior (Fig. 7b) where growth rates, expressed either as  $da/dt$  or  $da/dN$ , are higher at the lower frequency of loading, which implies that the fatigue mechanisms involved in this regime have a more significant cycle-dependence and lessened time-dependence.

## 4. Discussion

### 4.1. Cycle- vs. time-dependent crack growth

Several authors [2,6,12] have posed the question whether fatigue fracture in bone under cyclic loads is actually cycle- or time-dependent; their results, however, have invariably been inconclusive. One aim of the

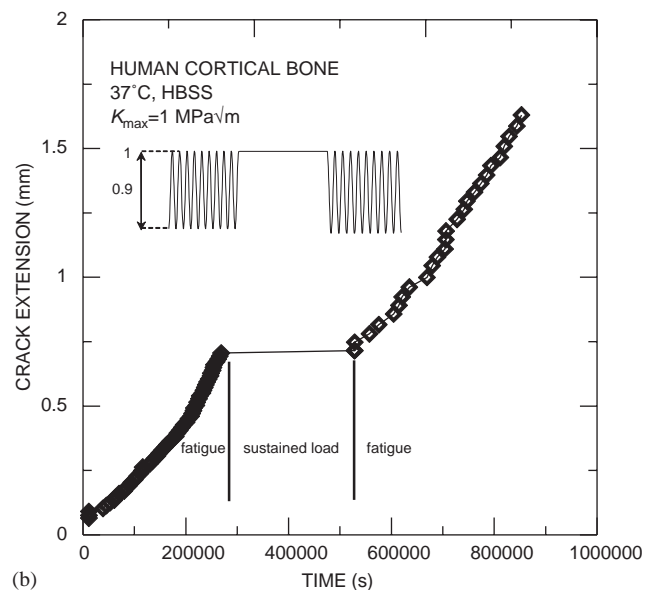
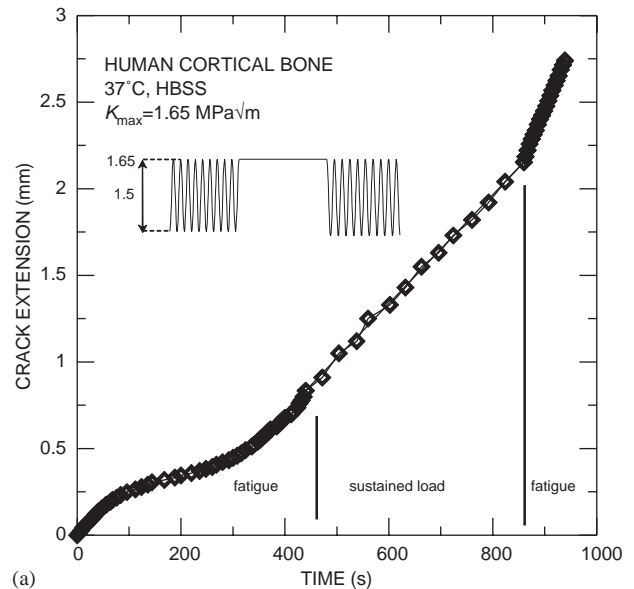


Fig. 6. Results of the “fatigue-sustained load-fatigue” tests at fixed  $K_{\text{max}}$  levels, presented as plots of crack extension as a function of time, for (a)  $K_{\text{max}} = 1.65 \text{ MPa}\sqrt{\text{m}}$ , (b)  $K_{\text{max}} = 1 \text{ MPa}\sqrt{\text{m}}$ .

present work has been to address this issue by focusing solely on crack-growth behavior and discerning whether the in vitro fatigue-crack propagation behavior measured in human cortical bone (Fig. 3) results from a true cyclic fatigue mechanism, or is simply caused by time-dependent, sustained-load cracking driven by the maximum load of the fatigue cycle.

We offer three approaches to help resolve this issue. The first of these is the constant  $K_{\text{max}}$  “fatigue-sustained load-fatigue” experiments shown in Fig. 6. The results of these experiments provide an unambiguous demonstration of a true cyclic fatigue effect in human cortical bone at low growth rates, specifically at  $K_{\text{max}} = 1.65 \text{ MPa}\sqrt{\text{m}}$  (Fig. 6b). This is apparent by examining the  $\Delta a$  vs.  $t$  data



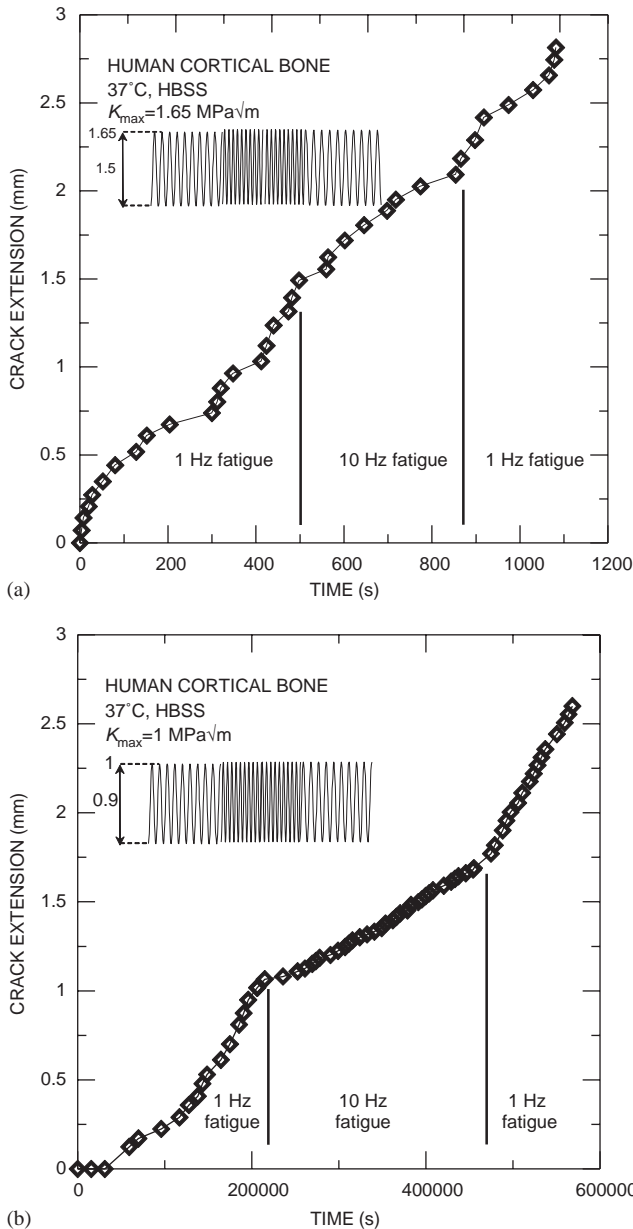


Fig. 7. Corresponding results for the variable frequency “1 Hz–10 Hz–1 Hz” tests at fixed  $\Delta K$  levels, presented as plots of crack extension as a function of time, for (a)  $\Delta K = 1.5 \text{ MPa}\sqrt{\text{m}}$  ( $K_{\text{max}} = 1.65 \text{ MPa}\sqrt{\text{m}}$ ), and (b)  $\Delta K = 0.9 \text{ MPa}\sqrt{\text{m}}$  ( $K_{\text{max}} = 1 \text{ MPa}\sqrt{\text{m}}$ ). Note the occurrence in (b) of faster crack-growth rates (both  $da/dt$  and  $da/dN$ ) at the lower frequency, which is in contrast to the behavior at high  $\Delta K$  levels, where the  $da/dt$  crack velocities are similar at 1 and 10 Hz.

at the end of the first (fatigue) block in Fig. 6b—holding the load constant at the fixed  $K_{\text{max}}$  level causes no crack extension; the crack will only continue to propagate if the loads are unloaded (and cycled). However, at higher growth rates, specifically at  $K_{\text{max}} = 1.65 \text{ MPa}\sqrt{\text{m}}$ , the effect is quite different (Fig. 6a); in this regime, the crack propagates subcritically under both sustained and cyclic loading at nominally similar rates. This would imply that subcritical crack-growth rates in bone at higher

stress intensities involves contributions from both time-dependent (“creep”) and cycle-dependent (fatigue) mechanisms, with static mechanisms dominating.

The second approach involves experiments where the frequency was changed, from 1 to 10 and back to 1 Hz, during cycling at constant  $\Delta K$ . It is apparent from these experiments (Fig. 7) that the significant time-dependent contribution to cracking, shown at high  $\Delta K$  by a  $da/dt$  crack velocity approximately independent of frequency, is reduced at low  $\Delta K$ , where crack-growth rates ( $da/dN$  and  $da/dt$ ) are lower at the higher frequency. As described in the introduction, such experiments where the frequency is changed rarely can give conclusive evidence concerning whether crack growth is cycle- or time-dependent; however, the results in Fig. 7 do clearly indicate that the time-dependent contribution to fatigue-crack propagation in bone is diminished in the low  $\Delta K$  regime.

Finally, in order to more fully characterize the range of driving forces over which cyclic effects dominate, a third approach is utilized whereby the cyclic fatigue-crack growth rates are “predicted” solely from sustained-load cracking data over the full range of  $K_{\text{max}}$  values (shown for human cortical bone in Fig. 1 [29]). The predictions are based on the methodology devised by Evans and Fuller [28] for materials that show *no true cyclic fatigue effects*, i.e., on the premise that there is no effect on crack extension specific to cyclic loading and that fatigue-crack growth is merely the sum of the increments of sustained-load (static) cracking associated with the maximum load of each fatigue cycle. Using this approach and integrating (with respect to time) over the fatigue loading cycle, we obtain:

$$\frac{da}{dN} = A \int_0^{1/f} \left[ \frac{1}{2}(K_{\text{max}} + K_{\text{min}}) + \frac{\Delta K}{2}(\sin(2\pi ft)) \right]^n dt, \quad (6)$$

where  $f$  is the cyclic test frequency,  $K_{\text{max}}$  and  $K_{\text{min}}$  are as previously defined, and  $A$  and  $n$  are the scaling constants as defined in Eq. (2). Thus, the “predicted” cyclic fatigue-crack growth rate behavior can be compared with that measured experimentally. If the “predicted” and experimental growth rates correspond well, the inference is that no true cyclic fatigue effect exists (for example, as seen in sapphire [30]); however, if at a fixed stress-intensity range the experimentally measured rates exceed the “predicted” rates, then this implies that cycle-dependent fatigue mechanisms are active.

Such a comparison between experimentally measured fatigue-crack growth rates in human cortical bone with the Evans-Fuller “predictions” solely from sustained-load cracking data are shown in Fig. 8. At low crack-growth rates ( $\sim 3 \times 10^{-10}$  to  $5 \times 10^{-7}$  m/cycle), the measured fatigue-crack growth rates (at a given  $K_{\text{max}}$ ) clearly exceed the predicted rates, whereas at higher growth rates ( $\sim 5 \times 10^{-7}$  to  $1 \times 10^{-5}$  m/cycle), the predicted rates are similar to slightly faster. This

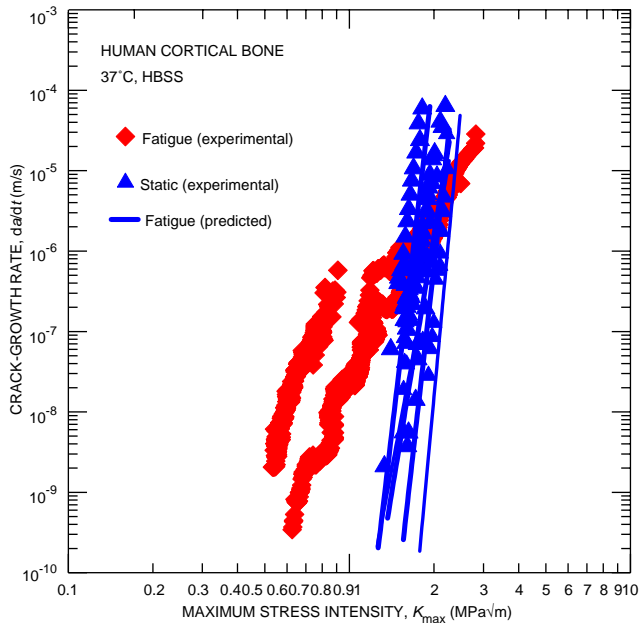


Fig. 8. Comparison of the experimental in vitro fatigue-crack growth rate results, expressed as  $da/dt$  as a function of  $K_{\max}$ , for human cortical bone with those predicted solely from sustained-load cracking data (Fig. 1), using the Evans and Fuller approach [28] (Eq. (4)). Note that experimentally measured growth rates in excess of the Evans-Fuller predictions, as shown for bone below  $\sim 10^{-6}$  m/cycle, implies the existence of a “true” cycle-dependent fatigue mechanism in this regime.

provides strong evidence that at low growth rates, a true cycle-dependent fatigue mechanism is operating in bone, whereas time-dependent sustained-load mechanisms appear to be more important at higher growth rates, the transition occurring between  $\sim 10^{-7}$  and  $10^{-6}$  m/cycle. These observations are entirely consistent with results of the “fatigue-sustained load-fatigue” and “1 Hz/10 Hz/1 Hz” experiments described above (Figs. 6 and 7). At low growth rates at a  $K_{\max}$  of  $1 \text{ MPa}\sqrt{\text{m}}$ , conditions are clearly below the transition and cycle-dependent mechanisms control fatigue-crack growth; a  $K_{\max}$  of  $1.65 \text{ MPa}\sqrt{\text{m}}$  is above the transition where sustained-load (static) mechanisms become active. This transition from static (“creep”-dominated) to cyclic (fatigue-dominated) mechanisms is similar to that suggested by Carter and Caler based on  $S/N$  data [7], and subsequently by Taylor [2], although the present study provides the first conclusive evidence of the effect, and establishes the stress-intensity range where this transition occurs.

#### 4.2. Mechanistic aspects of cortical bone fatigue

While there is clear evidence of a true cyclic fatigue effect in bone at growth rates below  $\sim 5 \times 10^{-7}$  m/cycle, the precise cycle-dependent mechanisms of crack advance are still uncertain. From the crack path observa-

tions (Fig. 4), it is apparent that cracks propagate preferentially along the weak cement lines. For sustained-load (static) fracture, it has been suggested that portions of the cement line fracture ahead of the advancing crack; as these “microcracks” attempt to link up with the main crack tip, uncracked ligaments can form (as shown in Fig. 4 (top panel)), leading to toughening via crack bridging [29]. Preferential cracking in the cement lines also acts to keep the crack tip sharp;<sup>5</sup> only at lower stresses, where the crack velocities are slower and the cement line remains intact ahead of the advancing crack, would there be sufficient time for crack-tip blunting to occur (Fig. 4—bottom panel). Under cyclic loading conditions, during the unloading portion of the fatigue cycle, such blunting would be “accommodated” by crack growth, e.g., some portion of the new surface area created by crack blunting on each cycle would become new crack area upon unloading. This process, which involves alternating blunting and resharping of the crack on each cycle, is the characteristic mechanism of fatigue-crack advance in ductile materials (e.g., in metals and polymers [38]). It is extremely difficult to confirm this mechanism by direct observation; nevertheless, since crack blunting is readily observable in cortical bone, as shown in Fig. 4 and also in Ref. [29], such a fatigue-crack advance mechanism would seem highly feasible.

Crack blunting in cortical bone [29], as in other mineralized tissues such as dentin [35], is time-dependent; consequently, one would expect some effect of cycle frequency on the crack-growth rates, as supported by the data shown in Fig. 7. A lower frequency implies that the crack has a longer time period to blunt on each cycle, requiring more “accommodation”, and consequently, a higher growth rate would be expected (blocks 1 and 3 in Fig. 7b). Such an effect has been observed in dentin [39], a mineralized tissue similar to bone, and provides support for a traditional (“metal-like”) alternating crack-tip blunting and resharping mechanism for fatigue-crack growth; however, the mechanism may be expected to be somewhat less effective in cortical bone where the time scales of blunting are substantially longer than in dentin [29]. However, this cycle-dependent mechanism would be consistent with the higher fatigue-crack growth rates as compared to the “predictions” based on the sustained-load cracking data.

It is also possible that fatigue-crack growth in bone also involves the cyclic-loading induced deterioration of the crack-bridging ligaments in the crack wake; this is a cyclic fatigue mechanism common to many ceramics

<sup>5</sup> It is interesting to note that (hydrated) dentin, which has a similar collagen/mineral structure to bone at the “molecular” level, displays significant crack blunting over much shorter time scales during sustained-load cracking [29,35]. It is reasoned that this occurs because there is no preferred crack path in dentin, akin to the cement lines in bone, to keep the crack tip sharp [29].

and brittle-matrix composites [40]. However, careful visual inspection of the crack wake using optical microscopy revealed that the surface lengths of the bridging zones, which are typically on the order of  $\sim 5$ – $6$  mm in bone [29], were comparable under cyclic and sustained loading, suggesting that this latter mechanism is probably not active in cortical bone.

#### 4.3. Fatigue lifetime predictions

With the availability of in vitro fatigue-crack growth-rate data for cortical bone (Fig. 3), conservative estimates of the expected fatigue life for cortical bone containing flaws/cracks of specific dimensions can be made, using a fracture-mechanics approach based on the notion that the life is comprised of the time or number of loading cycles for the largest pre-existing flaw to propagate to catastrophic failure. Such calculations clearly ignore the in vivo processes of repair and adaptation; indeed, the role of (fatigue) damage in inducing remodeling, e.g., repair by Basic Multicellular Units (BMU's), is well documented (e.g., [21,41,42]), as is the role of adaptation when bones change their geometry and mechanical properties to adapt to long-term changes in loading patterns (e.g., [2,43]). Nevertheless, the fracture-mechanics lifetime prediction is instructive as it provides a worst-case estimate of the life of bone in the presence of subcritical cracking. This is achieved by integrating the Paris crack-growth relationship in Eq. (2) (data in Table 1) between the limits of the initial flaw size,  $a_o$ , and the critical (final) flaw size,  $a_c$ , dictated by the fracture toughness (full details are given in Ref. [37] where the analysis has been applied to human dentin).

As a specific case, we consider the presence of an initial flaw  $100\ \mu\text{m}$  in size. Such flaws have been observed to occur both naturally and as a result of fatigue loading in cortical bone; indeed there are numerous studies that report incipient crack sizes of  $50$  to  $400\ \mu\text{m}$  (e.g., [21, 44–47]). For physiologically-relevant stresses between  $5$  and  $45\ \text{MPa}$ ,<sup>6</sup> predicted fatigue lifetimes range from over a billion cycles at a maximum stress of  $5\ \text{MPa}$  to an unrealistically low  $3000$  cycles at  $45\ \text{MPa}$ , clearly highlighting the critical role of bone remodeling/repair, particularly at high stresses. Such processes allow for bone to function at loading levels/conditions where the predicted in vitro fatigue lifetimes are negligible. Any excessive damage that the fatigue loading induces is repaired through remodeling and may be adapted for in the long run; indeed, it has

been suggested that bone remodeling to remove fatigue damage can allow for more gracile bones, with consequent skeletal weight savings [51].

#### 4.4. Other factors affecting fatigue in bone

There are a number of additional factors that may affect fatigue damage in bone which remain to be addressed. Although the test frequency of  $1\ \text{Hz}$  used in this study is within the range reported for common actions ( $0.5$ – $1.5\ \text{Hz}$ ), as most of these actions involve a range of frequencies [2,52], the full effect of frequency on fatigue-crack growth needs to be characterized. Similarly, how crack-growth behavior varies with orientation in bone has not been documented. More importantly, age and disease-induced alterations in the microstructure and composition of cortical bone would be expected to alter the kinetics of crack growth, yet this again has not been studied to date. In fact, the present study is limited to a rather small age group in order to remove any ambiguities that might be caused by such age-related changes in the mechanical behavior. It has been suggested that increased microdamage with aging leads to more extensive remodeling, resulting in a larger proportion of secondary osteons; as the difference in properties of the primary lamellar matrix and the secondary osteonal bone implies a stronger role for the cement lines (e.g., [21,53]), this suggests a mechanism by which the fatigue-crack growth behavior might change with age. It has also been proposed that excessive remodeling, rather than lower bone mass, is the primary cause of skeletal fragility associated with osteoporosis [54], giving added impetus to understanding what effect such conditions have on the fatigue properties of cortical bone. Finally, certain drugs (e.g., bisphosphonates) reduce the rate of bone turnover by curtailing the effect of the osteoclasts in the BMU's, and thus, the rate of repair of cracks in bone. The consequent increase in microcrack density would be expected to have a deleterious effect on the fatigue-crack growth behavior. Future work will seek to assess the effect of these factors from the perspective of developing a better understanding of the physical mechanisms associated with clinically-observed stress and fragility fractures.

## 5. Conclusions

Based on an investigation of the in vitro fatigue-crack growth behavior of hydrated human cortical bone in  $37^\circ\text{C}$  Hanks' Balanced Salt Solution in the proximal-distal direction, the following conclusions can be made:

1. The first cyclic fatigue-crack growth results for macroscopic cracks in human cortical bone are presented for a cyclic frequency of  $1\ \text{Hz}$  and display

<sup>6</sup>These choices are based on the stresses that are commonly experienced in vivo. Peak strains of  $350$ – $2100\ \mu\epsilon$  for typical activities have been reported for strain-gauge based measurements on the long bones (femur) in humans [2, 48–50]. A Young's modulus of  $12$ – $22\ \text{GPa}$  for secondary osteonal compact bone [2] implies that stress levels of  $\sim 5$ – $45\ \text{MPa}$  would be expected to be physiologically relevant.

- a Paris power-law dependency, i.e., crack-growth rates are proportional to a power-law function of the stress-intensity range, with an exponent of 4.4 to 9.5.
- Observations of the crack paths showed crack propagation to occur preferentially along the cement lines of the secondary osteons. Uncracked-ligaments bridges were observed to form in the crack wake; in addition, crack tips were seen to become progressively blunter with decreasing crack-growth rates.
  - Based on direct experimental evidence, it was unambiguously determined that a “true” cycle-dependent mechanism is active for fatigue-crack growth in cortical bone under cyclic loading conditions. Although crack extension at high crack-growth rates involves a significant contribution from time-dependent (“creep”) mechanisms, there is a definitive transition to cycle-dependent (fatigue) mechanisms with decrease in growth rates. By comparing measured fatigue-crack growth rates with those “predicted” by integrating sustained-load (static) cracking data over the course of the fatigue loading cycle, the transition was found to occur at  $\sim 5 \times 10^{-7}$  m/cycle, although this may be sensitive to the loading frequency.
  - A cycle-dependent mechanism for fatigue-crack advance in bone is suggested involving alternating blunting and resharpening of the crack tip (akin to that seen in ductile materials, such as metals and polymers). However, direct observation of this mechanism was not achieved, and further experiments are needed to conclusively determine the specific damage and crack advance micro-mechanisms involved.

### Acknowledgements

This work was supported by the National Institutes of Health under Grant No. 5R01 DE015633 (for RKN) and by the Director, Office of Science, Office of Basic Energy Science, Division of Materials Sciences and Engineering, Department of Energy under No. DE-Ac03-76SF00098 (for JJK and ROR). We also wish to thank Dr. A. P. Tomsia, University of California, San Francisco, CA for his support and Drs. C. Puttlitz and Z. Xu, San Francisco General Hospital, San Francisco, CA for supply of the human cortical bone.

### References

- Burr DB. Bone exercise and stress fractures. *Exerc Sport Sci Rev* 1997;25:171–94.
- Taylor D. Failure processes in hard and soft tissues. In: Milne I, Ritchie RO, Karihaloo BL, editors. *Comprehensive structural integrity: Fracture of materials from nano to macro*, vol. 9. Oxford, UK: Elsevier Inc.; 2003. p. 35–96.
- Iwamoto J, Takeda T. Stress fractures in athletes: Review of 196 cases. *J Orthop Sci* 2003;8:273–8.
- Meurman KO, Elfving S. Stress fracture in soldiers: a multifocal bone disorder. A comparative radiological and scintigraphic study. *Radiology* 1980;134:483–7.
- Lafferty JF, Raju PVV. The effect of stress frequency on the fatigue strength of cortical bone. *J Biomech Eng* 1979;101:112–3.
- Carter DR, Caler WE. Cycle-dependent and time-dependent bone fracture with repeated loading. *J Biomech Eng* 1983;105:166–70.
- Carter DR, Caler WE. A cumulative damage model for bone fracture. *J Orthop Res* 1985;3:84–90.
- Caler WE, Carter DR. Bone creep-fatigue damage accumulation. *J Biomech* 1989;22:625–35.
- Zioupos P, Wang XT, Currey JD. Experimental and theoretical quantification of the development of damage in fatigue tests of bone and antler. *J Biomech* 1996;29:989–1002.
- Choi K, Goldstein SA. A comparison of the fatigue behavior of human trabecular and cortical bone tissue. *J Biomech* 1992;25:1371–81.
- Zioupos P, Casinos A. Cumulative damage and the response of human bone in two-step loading fatigue. *J Biomech* 1998;31:825–33.
- Zioupos P, Currey JD, Casinos A. Tensile fatigue in bone: Are cycles-, or time to failure, or both, important? *J Theor Biol* 2001;210:389–99.
- Zioupos P, Wang XT, Currey JD. The accumulation of fatigue microdamage in human cortical bone of two different ages in vitro. *Clin Biomech* 1996;11:365–75.
- Currey JD. Mechanical properties of vertebrate hard tissues. *Proc Instn Mech Engrs* 1998;212H:399–412.
- Griffin LV, Gibelung JC, Martin RB, Gibson VA, Stover SM. The effects of testing methods on the flexural fatigue life of human cortical bone. *J Biomech* 1999;32:105–9.
- Vashishth D, Tanner KE, Bonfield W. Fatigue of cortical bone under combined axial-torsional loading. *J Orthop Res* 2001;19:414–20.
- Taylor D, O'Reilly P, Vallet L, Lee TC. The fatigue strength of compact bone in torsion. *J Biomech* 2003;36:1103–9.
- Pattin CA, Caler WE, Carter DR. Cyclic mechanical property degradation during fatigue loading of cortical bone. *J Biomech* 1996;29:69–79.
- Yeni YN, Fyhrie DP. Fatigue damage-fracture mechanics interaction in cortical bone. *Bone* 2002;30:509–14.
- Fleck C, Eifler D. Deformation behaviour and damage accumulation of cortical bone specimens from the equine tibia under cyclic loading. *J Biomech* 2003;36:179–89.
- Lee TC, Staines A, Taylor D. Bone adaptation to load: Microdamage as a stimulus for bone remodelling. *J Anat* 2002;201:437–46.
- Knott J. *Fundamentals of fracture mechanics*. London, UK: Butterworth & Co. (Publishers) Ltd.; 1976.
- Wright T, Hayes W. The fracture mechanics of fatigue crack propagation in compact bone. *Biomed Mater Res Symp (J Biomed Mater Res)* 1976;7(10):637–48.
- Gibelung JC, Shelton DR, Malik CL. Application of fracture mechanics to the study of crack propagation in bone. In: Niinomi M, Okaber T, Taleff, EM, Leuser DR, Lippard, HE, Editors. *Structural Biomaterials for the 21st Century*, TMS: Warrendale, PA; 2001.
- Suresh S, Ritchie RO. The propagation of short fatigue cracks. *Int Mater Reviews* 1984;29:445–76.
- Paris PC, Gomez MP, Anderson WP. A rational analytical theory of fatigue. *Trend Eng* 1961;13:9–14.
- Akkus O, Rimnac CM. Cortical bone tissue resists fatigue fracture by deceleration and arrest of microcrack growth. *J Biomech* 2001;34:757–64.

- [28] Evans AG, Fuller ER. Crack propagation in ceramic materials under cyclic loading conditions. *Metall Trans A* 1974;5:27–33.
- [29] Nalla RK, Kruzic JJ, Kinney JH, Ritchie RO. Mechanistic aspects of fracture and R-curve behavior in human cortical bone. *Biomaterials* 2004;26:217–31.
- [30] Asoo B, McNaney JM, Mitamura Y, Ritchie RO. Cyclic fatigue-crack propagation in sapphire in air and simulated physiological environments. *J Biomed Mater Res* 2000;52:488–91.
- [31] ASTM E647-00, in Annual Book of ASTM standards, vol. 03.01: Metals- mechanical testing; elevated and low-temperature tests; metallography. West Conshohocken, PA: ASTM; 2002, p. 595-635.
- [32] Behiri JC, Bonfield W. Orientation dependence on fracture mechanics of bone. *J Biomech* 1989;22:863–72.
- [33] Saxena A, Hudak Jr SJ. Review and extension of compliance information for common crack growth specimens. *Int J Fracture* 1978;14:453–68.
- [34] Murakami Y. (ed.) Stress intensity factor handbook, vol. 1. Elmsford, NY: Pergamon Press; 1987. 640.
- [35] Kruzic JJ, Nalla RK, Kinney JH, Ritchie RO. Crack blunting, crack bridging and resistance-curve fracture mechanics in dentin: effect of hydration. *Biomater* 2003;24:5209–21.
- [36] Imbeni V, Nalla RK, Bosi C, Kinney JH, Ritchie RO. In vitro fracture toughness of human dentin. *J Biomed Mater Res* 2003;66A:1–9.
- [37] Nalla RK, Imbeni V, Kinney JH, Staninec M, Marshall SJ, Ritchie RO. In vitro fatigue behavior of human dentin with implications for life prediction. *J Biomed Mater Res* 2003;66A:10–20.
- [38] Suresh S. *Fatigue of materials*, 2nd ed. Cambridge, UK: Cambridge University Press; 1998.
- [39] Kruzic JJ, Nalla RK, Kinney JH, Ritchie RO. Mechanistic aspects of in vitro fatigue-crack growth in dentin. *Biomaterials* 2004; 26, in press.
- [40] Ritchie RO. Mechanisms of fatigue crack propagation in metals, ceramics and composites: Role of crack tip shielding. *Mater Sci Eng* 1989;A103:15–28.
- [41] Burr DB, Martin RB, Schaffler M, Radin EL. Bone remodeling in response to in vivo fatigue microdamage. *J Biomech* 1985;18: 189–200.
- [42] Mori S, Burr DB. Increased intracortical remodeling following fatigue damage. *Bone* 1993;14:103–9.
- [43] Jones HH, Priest JD, Hayes WC, Tichenor CC, Nagel DA. Human hypertrophy in response to exercise. *J Bone Joint Surg* 1977;59A:204–8.
- [44] Burr DB, Stafford T. Validity of the bulk-staining technique to separate artifactual from in vivo bone microdamage. *Clin Orthop* 1990;260:305–8.
- [45] O’Brein FJ, Taylor D, Dickson GR, Lee TC. Visualisation of three-dimensional microcracks in compact bone. *J Anat* 2000;197:413–20.
- [46] Lee TC, Arthur TL, Gibson LJ, Hayes WC. Sequential labelling of microdamage in bone using chelating agents. *J Orthop Res* 2000;18:322–5.
- [47] Lee TC, Mohsin S, Taylor D, Parkesh R, Gunnlaugsson T, O’Brien FJ, Giehl M, Gowin W. Detecting microdamage in bone. *J Anat* 2003;203:161–72.
- [48] Burr DB, Milgrom C, Fyhrie D, Forwood M, Nyska M, Finestone A, Hoshaw S, Saiag E, Simkin A. In vivo measurement of human tibial strains during vigorous activity. *Bone* 1996;18:405–10.
- [49] Hillam RA. *Response of bone to mechanical load and alterations in circulating hormones*. Bristol, UK: University of Bristol; 1996.
- [50] Currey JD. How well are bones designed to resist fracture? *J Bone Mineral Res* 2003;18:591–8.
- [51] Martin RB. Fatigue damage, remodeling, and the minimization of skeletal weight. *J Theor Biol* 2003;220:271–6.
- [52] Whalen RT, Carter DR, Steele CR. Influence of physical activity on the regulation of bone density. *J Biomech* 1988;21:825–37.
- [53] Zioupos P. In vivo, in vitro and de novo microdamage in ageing human cortical bone and its effect on toughness. In: 12th Conference of European Society of Biomechanics. Dublin, Ireland: Royal Academy of Medicine in Ireland; 2000.
- [54] Heaney R. Is the paradigm shifting? *Bone* 2003;33:457–65.